

Published in final edited form as:

*Hypertension*. 2009 March ; 53(3): 556–563. doi:10.1161/HYPERTENSIONAHA.108.124594.

## Isoforms and Functions of NAD(P)H Oxidase at the Macula Densa

Rui Zhang<sup>1</sup>, Pamela Harding<sup>3</sup>, Jeffery L. Garvin<sup>3</sup>, Ramiro Juncos<sup>1</sup>, Ed Peterson<sup>4</sup>, Luis A. Juncos<sup>1,2</sup>, and Ruisheng Liu<sup>1,2,\*</sup>

<sup>1</sup>Department of Physiology & Biophysics University of Mississippi Medical Center, Jackson MS

<sup>2</sup>Division of Nephrology, Department of Medicine, University of Mississippi Medical Center, Jackson MS

<sup>3</sup>Hypertension and Vascular Research Division Henry Ford Hospital, Detroit MI

<sup>4</sup>Biostatistics and Research Epidemiology Henry Ford Hospital, Detroit MI

### Abstract

Macula densa cells produce superoxide ( $O_2^-$ ) during tubuloglomerular feedback primarily via NAD(P)H oxidase (NOX). The purpose of the present study was to determine NOXs expressed by the macula densa, and the role of each one in NaCl-induced  $O_2^-$  production. To identify which isoforms are expressed, we applied single cell RT-PCR to macula densa cells isolated by laser capture microdissection, and to MMDD1 cells (a macula densa-like cell line). The captured cells expressed nNOS (marker of macula densa), NOX2 and NOX4, but not NOX1. Expression of the NOXs and nNOS was essentially identical in the MMDD1 cells. Thus, we used MMDD1 cells to investigate which isoform is responsible for NaCl-induced  $O_2^-$  production. We used siRNA to knock down NOX2 or NOX4 in MMDD1 cells, and measured  $O_2^-$  exposed to low (LS; 70 mM NaCl) or high salt (HS; 140 mM NaCl) solutions. Exposing control cells (scrambled siRNA) to HS increased  $O_2^-$  concentrations from  $0.75 \pm 0.28$  to  $1.48 \pm 0.46$  units/min/ $10^5$  cells in LS and HS, respectively ( $p < 0.001$ ). Inhibiting NOX2 blocked the HS induced increase in  $O_2^-$  ( $0.62 \pm 0.39$  vs.  $0.76 \pm 0.31$  units/min/ $10^5$  cells in LS and HS groups, respectively). Blocking NOX4 did not affect HS-induced  $O_2^-$  levels.  $O_2^-$  levels in the control cells during LS and HS were  $0.80 \pm 0.30$  and  $1.56 \pm 0.49$  units/min/ $10^5$  cells, respectively ( $p < 0.001$ ); whereas  $O_2^-$  levels in NOX4-siRNA treated cells during LS and HS were  $0.40 \pm 0.25$  and  $1.26 \pm 0.51$  units/min/ $10^5$  cells, respectively ( $p < 0.001$ ). We conclude that while macula densa cells express the NOX2 and NOX4 isoforms, NOX 2 is primarily responsible for NaCl-induced  $O_2^-$  generation.

### Keywords

NAD(P)H oxidase; superoxide; macula densa; tubuloglomerular feedback

Macula densa cells are modified epithelial cells located at the end portion of the thick ascending limb, at the hilus of its own glomerulus where they are in close contact with the glomerular arterioles. In response to changes in luminal NaCl delivery, they initiate signaling pathways that adjust glomerular filtration rate (a process called tubuloglomerular feedback; TGF), and regulate renin release. These two processes are amongst the most important mechanisms that regulate the renal microcirculation and sodium excretion<sup>1-3</sup>; consequently, they are tightly regulated by various factors such as angiotensin II, nitric oxide and superoxide ( $O_2^-$ ).

\*Corresponding author: Ruisheng Liu, MD, PhD Department of Physiology & Biophysics University of Mississippi Medical Center 2500 N. State St., Jackson MS 39216 Phone: 601-815-9501 FAX: 601-984-1817 e-mail: E-mail: rliu@physiology.umsmed.edu. Current address of R. Zhang: Shandong Medical College, Jinan, China

Disclosures None.

$O_2^-$  is produced by various cytosolic enzymes and by mitochondria. The major source of  $O_2^-$  in the kidney is NAD(P)H oxidase<sup>4, 5</sup>, which is present in the vasculature, cortex and medulla<sup>6-9</sup>, and has been implicated in the pathogenesis of several models of hypertension<sup>10</sup>. Renal NAD(P)H oxidase activity is increased by angiotensin II and by salt loading<sup>11</sup>. Macula densa cells have been found to have main units of NAD(P)H oxidase<sup>12</sup> and produce  $O_2^-$  in response to increased NaCl delivery<sup>6, 13</sup>. Macula densa-derived  $O_2^-$  can modulate single nephron glomerular filtration rate during infusion of angiotensin II<sup>14</sup>, and we recently reported that  $O_2^-$  in the macula densa augments the TGF response, primarily by scavenging nitric oxide<sup>6</sup>. Accordingly,  $O_2^-$  is an important modulator of TGF, renal hemodynamics and sodium excretion. However, which isoforms of NAD(P)H oxidase (NOXs) are produced at the macula densa cells and the function of each isoform are unknown. Performing such studies has been difficult because macula densa cells represent a very small percentage of renal cells and are located in very small clusters. However, the recent development of laser capture microdissection (LCM)<sup>15-17</sup>, a novel technique that facilitates separating and harvesting of specific cells, now allows us to isolate and study specific renal cells, including macula densa cells.

In the present study, we isolated macula densa cells from frozen rat kidney using LCM. We identified the NOXs expressed by these captured macula densa cells and compared them to those expressed by a macula densa-like cell line (MMDD1). In addition, we investigated which isoform is responsible for NaCl-induced  $O_2^-$  generation in the macula densa. We found that captured macula densa and MMDD1 cells express NOX2 and NOX4, and that the NOX2 is the isoform primarily responsible for NaCl-induced  $O_2^-$  production by the macula densa.

## MATERIALS AND METHODS

All experiments were approved by the Henry Ford Hospital Animal Care and Use Committee prior to performing any procedures on animals. Studies were performed in accordance with the Guide for the Care and Use of Laboratory Animals (NIH publication 92-93) and the Guidelines of the Animal Welfare Act. Experiments were undertaken on renal tissue obtained from male Sprague-Dawley rats, and in MMDD1 cells, a renal epithelial cell line with properties of macula densa cells (kindly provided by Dr. Schnermann, NIH). All chemical compounds were purchased from Sigma, except DMSO and lucigenin which were obtained from Invitrogen (Eugene, OR).

### LCM of Macula Densa Cells

Sprague-Dawley rats weighing between 100-120 g were anesthetized with ketamine (50 mg/kg i.p.) and xylazine (50 mg/kg i.p.). The abdomen was opened and the kidneys removed. Sections of kidney were snap-frozen in optimal cutting temperature (O.C.T) medium using an isopentane bath, and 8  $\mu$ m frozen sections were stained and dehydrated using a Histogene frozen section staining kit (Arcturus) according to the manufacturer's instructions. The sections were then viewed with the LCM microscope. The macula densa cells, which were identified by their anatomical location and morphology, were then "painted" (marked on computer screen) and dissected with the laser under the  $\times 20$  objective, using a beam width of 7.5  $\mu$ m and a beam intensity of 50 mW. We subsequently used RT-PCR to measure the NOX expression in the captured cells, and of nNOS a marker for macula densa cells<sup>18</sup> to confirm that the captured cells were macula densa.

### MMDD1

We used MMDD1 cells, a renal epithelial cell line with properties of macula densa cells, developed and kindly supplied by Dr. Schnermann (NIH)<sup>19</sup>. These cells were derived from SV40 transgenic mice and acquired using fluorescence-activated cell sorting of renal tubular

cells labeled with segment-specific lectins. This cell line has been shown to express well-known macula densa markers, such as cyclooxygenase 2 (COX-2), nNOS, ROMK, and NKCC2 19-21. In the present studies, MMDD1 cells at passages 15-20 were routinely trypsinized and suspended in DMEM nutrient mixture- Ham's F-12 (DMEM/F-12) supplemented with 10% fetal bovine serum, penicillin (100 U/ml), and streptomycin (100 µg/ml). The cells were plated onto culture dishes and incubated at 37°C in a humidified atmosphere of 95% room air-5% CO<sub>2</sub>. The media was changed every 2 days, and once the cells reached confluence (typically in 3-4 days), the cells were ready for siRNA and O<sub>2</sub><sup>-</sup> experiments.

### RT-PCR for macula densa cells isolated by LCM

We used the single-cell-RT-PCR kit (Ambion) as described below. Despite the potential for measuring mRNA from single cells, our pilot experiments suggested that at least 20 cells captured from the frozen slide were required in order to extract enough mRNA for RT-PCR. Total RNA was extracted using a PicoPure RNA isolation kit (Arcturus) according to the manufacturer's instructions. Five µl of RNA was reverse transcribed for 30 minutes at 45°C using 50 µM random primers (Invitrogen) and a MessageSensor RT Kit (Ambion), then heated for 10 minutes at 95°C and subsequently placed on ice. The resultant RT product was then amplified by PCR using the following protocol. Five µl of RT product and 0.5 µM gene-specific primers were added to 1 unit SuperTaq (Ambion) and heated to 95°C for 5 minutes. The samples were then cycled 40 times as follows: 15 seconds at 95°C, 30 seconds at 58°C, and 1 minute at 72°C. The final extension was for 10 minutes at 72°C.

### RT-PCR for MMDD1 Cells

Total RNA was extracted using RNeasy Micro Kit (Qiagen) according to the manufacturer's instructions. Briefly, 0.5 µg of total RNA was reverse transcribed for 1 hour at 37°C using 10 µM random primers (Invitrogen) and a Omniscript RT Kit (Qiagen). The resultant RT product was then amplified by PCR by adding 5 µl of the RT reaction and 1 µM of the gene-specific primers to the PCR master Mix Kit (Promega). The mixed samples were then heated to 94°C for 5 min and cycled at 94°C for 45 sec, 58°C for 45 sec, 72°C for 1 min for 35 cycles. Final extension was for 10 min at 72°C.

The amplified products of the Single-Cell-RT-PCR and MMDD1-RT-PCR were run on 1.5% agarose gels containing ethidium bromide (0.5 µg/ml) and visualized under UV light. GAPDH, as a house-keeping gene, was set up as an internal loading control. All steps for reverse transcription and PCR are the same according to the manufacturer's instruction. Samples which were not reverse-transcribed were used as a negative control and samples from kidney cortex were used as a positive control. A 100-bp DNA ladder marker was used to identify the molecular weight of the targeted DNA. Primer sequences, expected band and GenBank number are listed in table 1.

### Preparations for small interfering RNA (siRNA)

All siRNAs were designed and synthesized by Santa Cruz. siRNA transfection was performed using a siRNA Reagent System (Santa Cruz) according to the manufacturer's instructions. Scrambled siRNA were synthesized and used as negative controls. To achieve optimal transfection efficiency, various parameters, including the amounts of transfection reagent, RNA, and TransMessenger-RNA complexes, the cell density, and the length of exposure of cells to TransMessenger-RNA complexes, were optimized. At 24 h before transfection, MMDD1 were transferred onto 6-well plates ( $5 \times 10^5$  cells per well) and transfected with 0.8 µg of each siRNA duplex using TransMessenger transfection reagent for 4 h in medium devoid of serum and antibiotics. This procedure does not affect cell viability. Macula densa cells were washed once with PBS and grown in complete medium. Gene silencing were monitored by measuring RNA after incubation for 24 to 72 h.

## Measurement of O<sub>2</sub><sup>-</sup> with lucigenin

We measured O<sub>2</sub><sup>-</sup> production in MMDD1 cell line using a lucigenin-enhanced chemiluminescence assay as previously described<sup>22-24</sup>. Briefly, confluent MMDD1 cells were rinsed twice in PBS solution. The cells were then trypsinized and suspended in 5 ml containing either high or low NaCl solutions. The high NaCl solution contained (in mM): 140 NaCl, 10 HEPES, 1.0 CaCO<sub>3</sub>, 0.5 K<sub>2</sub>HPO<sub>4</sub>, 4.0 KHCO<sub>3</sub>, 1.2 MgSO<sub>4</sub>, 5.5 glucose, 0.5 Na acetate, 0.5 Na lactate, and pH 7.4. The low NaCl solution was the same as high NaCl solution except that the NaCl was reduced to 70 mM and mannitol was used to maintain the same osmolarity as the high NaCl solution. Lucigenin (5 μM) was added to each of the samples, which was then placed in 1.6-ml polypropylene 8 × 50-mm tubes (Evergreen Scientific, Los Angeles, CA). After allowing the samples to equilibrate with lucigenin at 37°C for 15 min, the tubes were placed in a luminometer (TD-20e; Turner Designs, Sunnyvale, CA) with the light chamber maintained at 37°C. Luminescence measurements were integrated for 30-s periods and the cycle repeated 9 times, averaging 10 values. At the end of each experiment, the cell-permeant O<sub>2</sub><sup>-</sup> scavenger Tiron (10 mM) was added and 15 more cycles read; the final 8 values were averaged. O<sub>2</sub><sup>-</sup> was expressed by units/min/×10<sup>5</sup> cells. All O<sub>2</sub><sup>-</sup> measurements were performed in the presence of 10<sup>-4</sup>M N-nitro-L-arginine methyl ester, a NOS inhibitor, to eliminate O<sub>2</sub><sup>-</sup> quenching by nitric oxide.

## Statistics

We used a two-way analysis of variances (ANOVA) to assess if a NOX or the level of salt affected O<sub>2</sub><sup>-</sup> production and whether the NOX affects salt-induced changes. The design had two main effects, NOX and salt concentration, and one two-way interaction. If the interaction was significant we checked for salt effects using paired t-tests on each isoform separately and for NOX effects using student's t-tests on each salt concentration separately.

The examination of three repeated measures was accomplished with ANOVA for repeated measures. The interest in this analysis was primarily directed at the three pairwise comparisons. These were done using paired t-tests with a Hochberg's adjustment for multiple testing. Data are expressed as the means plus or minus the standard error and an adjusted p-value less than 0.05 was considered significant.

## RESULTS

### NOXs expressed in LCM-captured macula densa and MMDD1 cells

We first demonstrated the feasibility of isolating and capturing macula densa cells using LCM. Figure 1 shows a representative example of a glomerulus with its macula densa, before and after the macula densa has been captured with LCM; the isolated macula densa cells are shown in Panel C of Figure 1. As seen in the figure, macula densa cells were readily identifiable by their anatomic location and morphology. These captured cells expressed nNOS (see below and Figure 2), but not eNOS (expressed by the thick ascending limb and vasculatures) thus further confirming that the captured cells were macula densa cells and not contaminated by surrounding cells.

We next used RT-PCR techniques to identify which NOXs are expressed by the macula densa cells. Figure 2 shows representative blots for the NOX1, NOX2 and NOX4 isoforms, as well as for nNOS, in renal cortex, laser-captured macula densa cells, and MMDD1 cells. Figure 2A shows that the macula densa cells collected using LCM clearly expressed the NOX2 and NOX4, as well as nNOS (they did not express NOX1), indicating that NOX2 and NOX4 are the main isoforms present in macula densa cells.

Because the MMDD1 cell line may have some differences with macula densa cells isolated from in vivo renal cortex, yet we would be using this cell line to study the function of each NOX in these cells, we tested whether the MMDD1 cells expressed the same NOXs as the laser-captured macula densa cells. The representative blot depicted in Figure 2B shows that the expression profile for the NOXs and nNOS in the MMDD1 cells was essentially identical to that of the laser-captured macula densa cells. Thus, these results demonstrate that the laser-captured macula densa cells and MMDD1 cells exhibit the same NAD(P)H oxidase expression profile, and together they provide strong evidence that macula densa cells express the NOX2 and NOX4 isoforms.

Figure 2C shows that the renal cortex expressed all 3 NOXs and nNOS, thus verifying the efficacy of all of our primers to detect the NOXs and nNOS.

### Comparative function of macula densa-derived NOX2 and NOX4

To study the functions of individual NOX, we used siRNA to knockdown NOX2 and NOX4 mRNA, in MMDD1 cell line. We first determined the efficacy of the siRNA in reducing their target NOX mRNA. Figure 3A shows a representative blot for NOX2 mRNA in MMDD1 cells with the siRNA-NOX2 or the scramble siRNA control; whereas Figure 3B shows an analogous blot for NOX4 mRNA. The bottom graphs in these figures show the corresponding densitometric data. Incubating the MMDD1 cells for 48 hours with 0.8  $\mu$ g of siRNA duplex transfection reagent was very effective at knocking down the mRNA of its intended target; the siRNA-NOX2 knocked down NOX2 mRNA by  $91 \pm 0.5\%$ , NOX2 mRNA knocked down by NOX4-siRNA mRNA only by  $6 \pm 5.1\%$  (as compared to scramble NOX2; Fig 3) and the siRNA-NOX4 knocked down NOX4 mRNA by  $86 \pm 2.1\%$ . To test the specificity of the siRNAs we used, we measured NOX2 mRNA in siRNA-NOX4 treated cells and measured NOX4 mRNA in siRNA-NOX2 treated cells. In siRNA-NOX4 treated cells, NOX2 mRNA was  $94.5 \pm 5.2\%$  compared with the cells treated with scrambled siRNA. In siRNA-NOX2 treated cells, NOX4 mRNA was  $103.1 \pm 5.6\%$  compared with the control (Figure 3;  $n = 5$ ). Accordingly, we used this dose and incubation time in the remaining experiments.

One of the primary stimuli for NOX-derived  $O_2^-$  production in macula densa cells is the increased luminal NaCl. To determine which NOX isoform is responsible for this increase in  $O_2^-$ , we tested whether knocking down either NOX2 or NOX4 mRNA in MMDD1 cells prevented high NaCl-induced increases in  $O_2^-$ . The effect of the knocking down NOX2 on  $O_2^-$  concentrations levels in MMDD1 cells is shown in Figure 4. A high NaCl solution caused  $O_2^-$  concentration to increase in control MMDD1 cells (treated with scrambled NOX2 siRNA); the  $O_2^-$  concentration was  $0.88 \pm 0.11$  and  $1.74 \pm 0.17$  units/min/ $10^5$  cells in the low (70 mM) and high (140 mM) NaCl solutions, respectively ( $p < 0.001$ ). Knocking down NOX2, did not alter basal  $O_2^-$  levels, but blocked high NaCl-induced increases in  $O_2^-$  ( $O_2^-$  concentrations were  $0.73 \pm 0.20$  and  $0.90 \pm 0.15$  units/min/ $10^5$  cells in the low and high NaCl solutions, respectively;  $n = 7$ ). On the other hand, knocking down NOX4 had no effect on high NaCl-induced  $O_2^-$  production (Figure 5). The  $O_2^-$  concentration in the control cells (treated with scrambled NOX4 siRNA) was  $0.94 \pm 0.12$  and  $1.82 \pm 0.17$  units/min/ $10^5$  cells in the low and high NaCl groups, respectively ( $p < 0.001$ ). The high NaCl solution caused a similar increase in  $O_2^-$  concentration in NOX4 siRNA treated cells;  $O_2^-$  was  $0.51 \pm 0.12$  and  $1.58 \pm 0.24$  units/min/ $10^5$  cells in the low and high NaCl groups, respectively ( $p < 0.001$ ;  $n = 9$ ). These data indicate that NOX2 is the primary isoform responsible for NaCl-induced  $O_2^-$  generation in the macula densa and NOX4 is an isoform responsible for basal  $O_2^-$  generation.

We previously reported NaCl-induced  $O_2^-$  generation in isolated perfused MD cells is mainly due to NAD(P)H oxidase<sup>13, 25</sup>. To establish whether NAD(P)H oxidase was also the main source of  $O_2^-$  in MMDD1 cells, we determined the relative contribution of NAD(P)H oxidase, xanthine oxidase and cyclooxygenase-2 (COX-2) to NaCl-induced  $O_2^-$  generation in MMDD1

using antagonist of NAD(P)H oxidase, xanthine oxidase and cyclooxygenase-2 (COX-2)(Fig 6). First, we tested the role NAD(P)H oxidase in NaCl induced  $O_2^-$  generation in MMDD1. The  $O_2^-$  concentration in MMDD1 cells on low and high NaCl solution was  $0.50 \pm 0.05$  and  $1.36 \pm 0.09$  units/ $10^5$ cells ( $n = 7$ ;  $p < 0.01$ ). Adding the NAD(P)H oxidase inhibitor, apocynin ( $10^{-5}$  M), for 30 minutes to high NaCl MMDD1 cells caused the  $O_2^-$  concentration to decrease to  $0.68 \pm 0.05$  units/ $10^5$ cells ( $n = 19$ ;  $p < 0.01$ ). Thus, blocking NAD(P)H oxidase blunted NaCl-induced increases in  $O_2^-$  concentration, suggesting that NAD(P)H is an important source of  $O_2^-$  production in these cells. In contrast, blocking xanthine oxidase with oxypurinol did not significantly alter  $O_2^-$  concentrations. In these experiments, the  $O_2^-$  concentrations in the cells maintained in low and high NaCl solutions were  $0.59 \pm 0.05$  and  $1.32 \pm 0.12$  units/ $10^5$ cells, respectively ( $p < 0.001$ ), and  $1.14 \pm 0.12$  units/ $10^5$ cells in the cells treated with oxypurinol ( $10^{-4}$  M) for 30 minutes. Finally, blocking COX-2 with NS-398 also did not affect NaCl-induced increase in MMDD1  $O_2^-$  concentration.  $O_2^-$  concentrations were  $0.52 \pm 0.03$  and  $1.36 \pm 0.09$  units/min/ $10^5$ cells during low and high NaCl solutions, respectively ( $n = 14$ ;  $p < 0.01$ ), and  $1.25 \pm 0.09$  units/min/ $10^5$ cells in the cells treated with NS-398 ( $10^{-6}$  M) for 30 minutes. These data indicate that NaCl-induced increases in  $O_2^-$  in MMDD1 cells, like that in freshly isolated and perfused macula densa cells, is predominantly via NAD(P)H oxidase<sup>13, 25</sup>.

## DISCUSSION

In the present study we successfully applied LCM to isolate macula densa cells from frozen rat kidney cortex. These cells expressed NOX2 and NOX4, but not NOX1. This expression profile was essentially identical to that of the MMDD1 cells, further verifying the similarity of these two cell types and their suitability for macula densa research. Finally, using the MMDD1 cells, we found that the NOX2 is the main source of NaCl-induced  $O_2^-$  and NOX4 is responsible for basal  $O_2^-$  production.

The macula densa plays a major role in NaCl-dependent regulation of glomerular arteriolar tone and renin release, and thus have been the subject of much study<sup>18, 26, 27</sup>. However, it is difficult to acquire macula densa cells in quantities sufficient enough to perform the necessary biochemical analysis required to study cellular and molecular mechanisms. The recent development of LCM provides us with a tool that can be used to isolate macula densa<sup>15</sup>. LCM is a novel technique based on the adherence of visually selected cells to a thermoplastic membrane (overlying the dehydrated tissue section), which is focally melted by triggering a low-energy infrared laser pulse. The melted membrane forms a composite with the selected tissue area that is removed by simply lifting off the membrane. The size of the laser spot can be selected as 30, 15 or 7.5  $\mu$ m, facilitating dissection of groups of cells or even single cells. Consequently, LCM can be applied to a wide range of cell and tissue preparations, including frozen tissue sections<sup>16, 17</sup>. The first objective of the present study was to use LCM to harvest macula densa cells from frozen rat kidneys. We identified macula densa cells in the tissue sections, and found that we were readily able to dissect and harvest them using LCM. We then confirmed that the captured cells were macula densa cells by verifying that they expressed nNOS<sup>18</sup>, demonstrating that LCM can be used effectively to harvest macula densa cells. Thus we next used LCM-harvested macula densa cells to investigate the source of NaCl-induced  $O_2^-$  generation.

Emerging evidence suggests that  $O_2^-$  produced by the macula densa plays an important role in regulating TGF. We reported recently that increasing tubular NaCl induces  $O_2^-$  production by the macula densa primary from NAD(P)H oxidase.  $O_2^-$  produced by the macula densa segment TGF by scavenging nitric oxide<sup>6</sup>. This contention is further supported by Chabrashvili et al. who found that the macula densa expresses the main components of NAD(P)H oxidase, some of which are overexpressed in the SHR<sup>12</sup>, an experimental model of hypertension that has enhanced oxidant stress and TGF. These studies indicate the existence and functional

importance of NAD(P)H oxidase at the macula densa cells. However, they did not establish which NOX(s) are responsible for macula densa-derived  $O_2^-$ . Five isoforms of NOX proteins with distinct tissue distributions have been found: NOX1 is expressed mainly in the colonic epithelium and vascular smooth muscle cells<sup>28-30</sup>, NOX2 (gp91<sup>phox</sup>) in phagocytes, NOX3 in the embryonic kidney<sup>31</sup>, NOX4 in the renal cortex<sup>32, 33</sup>, and NOX5 in T- and B-lymphocytes of the spleen and lymph nodes as well as sperm precursors in the testis<sup>34</sup>. Recently, two new members of the gp91<sup>phox</sup>-homologue family have been reported<sup>35</sup>, dual oxidase (DUOX) 1/thyroid oxidase 1, found primarily in the thyroid and lung; and DUOX2/thyroid oxidase 2, primarily located in the thyroid and colon<sup>36, 37</sup>. The potential NAD(P)H oxidase isoforms expressed in the adult kidney are NOX1, NOX2 and NOX4, since NOX3, NOX5 and DUOX are not likely to be present<sup>31, 34-36</sup>. We tested for the presence of these three isoforms in the macula densa. Our RT-PCR studies in renal cortex confirmed the presence of the 3 isoforms. Of these, only NOX2 and NOX4 were expressed in the LCM-captured macula densa cells. Likewise, these same two isoforms were expressed in a similar manner in the MMDD1 cells, providing substantiate that MMDD1 cells are suitable to study  $O_2^-$  generation of the macula densa. The major reason we choose MMDD1 cell line is because it is difficult to knockdown NOX2 and NOX4 at the macula densa *in vivo*.

We next used the MMDD1 cells to investigate which NOX is responsible for NaCl-induced  $O_2^-$  production. We arbitrarily set low and high NaCl solution as 70 and 140 mM NaCl according to literature<sup>19</sup>, in which they found that low NaCl stimulates prostaglandin E2 release, cyclooxygenase-2 expression and activation of MAP kinases. We blocked the expression of either NOX2 or NOX4 with a specific siRNA and measured  $O_2^-$  concentration during exposure to low and high NaCl solutions. Our data indicates that NOX2 is the primary source of  $O_2^-$  at the macula densa induced by NaCl. While they do not rule out that NOX4 may contribute significantly during other conditions, it does not seem to play a role in NaCl-induced  $O_2^-$  production. These results are consistent with our previous study in which we found that NaCl-induced  $O_2^-$  production in the macula densa cells was blocked by apocynin, a NAD(P)H oxidase inhibitor that acts by blocking serine phosphorylation of the cytosolic p47<sup>phox</sup> subunit. Our present study has established that while NOX4 contribute to basal  $O_2^-$  production in the macula densa, NOX2 is the primary source for  $O_2^-$  induced by NaCl.

The different roles for the NOXs are not unexpected for the following reasons. Firstly, NOX2 and NOX4 localize to different subcellular compartments<sup>38, 39</sup>. Because  $O_2^-$  cellular signaling likely depends on both the amount and site of  $O_2^-$  production<sup>38, 40, 41</sup>, it seems likely that NOX2 and NOX4 may mediate distinct signaling pathways. In addition, they are regulated differently. Activation of NOX2 requires agonist stimulation to induce translocation of cytoplasmic proteins to the plasma membrane and RAC activation, raising the possibility that angiotensin II-induced enhancement of macula densa  $O_2^-$  production (and TGF) may also be via NOX2. Conversely, NOX4 is not controlled by RAC or the known cytosolic NOX components, and does not require or utilize the NOX1-associated proteins, NOXO1 and NOXA1. NOX4 has been reported to co-localize with p22<sup>phox</sup> to internal membranes and constitutive active<sup>41</sup>. Hence, the mechanisms by which macula densa NOX4 expression and function is regulated, and its biological significance remain unknown. Carouandel and his colleagues showed that when nNOS is studied under depleted arginine conditions, blockade with arginine derivatives dictates  $O_2^-$  production<sup>42</sup>. In present study, we cannot exclude the possibility of enhanced  $O_2^-$  production from nNOS in MMDD1 cells when we used L-NAME. However, we believe the  $O_2^-$  from nNOS is not significant, since inhibition of NAD(P)H oxidase with apocynin blocks  $O_2^-$  production (see Fig 6).

In summary, we found that NOX2 and NOX4 are the isoforms of NOD(P)H oxidase expressed at the macula densa. NOX2 is the primary source of  $O_2^-$  induced by NaCl, whereas NOX4 is responsible for basal  $O_2^-$  production.

## Perspective

We used a novel approach that combined LCM of macula densa cells with functional studies in MMDD1 cells, a macula densa-like cell line, to facilitate the study of macula densa cellular function. We applied LCM to isolate and harvest macula densa cells from frozen kidney tissue and then identified that these captured macula densa cells express the NOX2 and NOX4 isoforms of NAD(P)H oxidase. The expression profile of these cells was essentially the same as that of the MMDD1 cells, a macula densa-like cell line. The NOX2 is the main source for NaCl-induced  $O_2^-$ , whereas the NOX4 contribute to the basal  $O_2^-$  production. Thus conditions in which the activity of either of these NOXs is altered may contribute to enhanced TGF and abnormal NaCl homeostasis.

## Acknowledgments

**Sources of Funding:** This work was supported by the National Institutes of Health Grants RO1-HL086767 (to R. Liu) and RO1-DK073401 (to L.A. Juncos).

## Reference List

- (1). Wilcox CS, Welch WJ, Murad F, Gross SS, Taylor G, Levi R, Schmidt HHW. Nitric oxide synthase in macula densa regulates glomerular capillary pressure. *Proc Natl Acad Sci USA* 1992;89:11993–11997. [PubMed: 1281548]
- (2). Schnermann J, Persson AE, Agerup B. Tubuloglomerular feedback. Nonlinear relation between glomerular hydrostatic pressure and loop of Henle perfusion rate. *J Clin Invest* 1973;52:862–869. [PubMed: 4693650]
- (3). Persson AEG, Salomonsson M, Westerlund P, Greger R, Schlatter E, Gonzalez E. Macula densa cell function. *Kidney Int* 1991;39:S-39–S-44.
- (4). Wilcox CS. Oxidative stress and nitric oxide deficiency in the kidney: a critical link to hypertension? *Am J Physiol Regul Integr Comp Physiol* 2005;289:R913–R935. [PubMed: 16183628]
- (5). Gill PS, Wilcox CS. NADPH oxidases in the kidney. *Antioxid Redox Signal* 2006;8:1597–1607. [PubMed: 16987014]
- (6). Liu R, Ren Y, Garvin JL, Carretero OA. Superoxide enhances tubuloglomerular feedback by constricting the afferent arteriole. *Kidney Int* 2004;66:268–274. [PubMed: 15200433]
- (7). Mitchell KD, Navar LG. Enhanced tubuloglomerular feedback during peritubular infusions of angiotensins I and II. *Am J Physiol* 1988;255:F383–F390. [PubMed: 3414799]
- (8). Modlinger P, Chabrashvili T, Gill PS, Mendonca M, Harrison DG, Griendling KK, Li M, Raggio J, Wellstein A, Chen Y, Welch WJ, Wilcox CS. RNA silencing in vivo reveals role of p22<sup>phox</sup> in rat angiotensin slow pressor response. *Hypertension* 2006;47:238–244. [PubMed: 16391171]
- (9). Mundel P, Bachmann S, Bader M, Fischer A, Kummer W, Mayer B, Kriz W. Expression of nitric oxide synthase in kidney macula densa cells. *Kidney Int* 1992;42:1017–1019. [PubMed: 1280698]
- (10). Harrison DG, Cai H, Landmesser U, Griendling KK. Interactions of angiotensin II with NAD(P)H oxidase, oxidant stress and cardiovascular disease. *J Renin Angiotensin Aldosterone Syst* 2003;4:51–61. [PubMed: 12806586]
- (11). Kitiyakara C, Chabrashvili T, Chen Y, Blau J, Karber A, Aslam S, Welch WJ, Wilcox CS. Salt intake, oxidative stress, and renal expression of NADPH oxidase and superoxide dismutase. *J Am Soc Nephrol* 2003;14:2775–2782. [PubMed: 14569087]
- (12). Chabrashvili T, Tojo A, Onozato ML, Kitiyakara C, Quinn MT, Fujita T, Welch WJ, Wilcox CS. Expression and cellular localization of classic NADPH oxidase subunits in the spontaneously hypertensive rat kidney. *Hypertension* 2002;39:269–274. [PubMed: 11847196]
- (13). Liu R, Garvin JL, Ren Y, Pagano PJ, Carretero OA. Depolarization of the macula densa induces superoxide production via NAD(P)H oxidase. *Am J Physiol Renal Physiol* 2007;292:1867–1872.
- (14). Nouri P, Gill P, Li M, Wilcox CS, Welch WJ. p22<sup>phox</sup> in the macula densa regulates single nephron GFR during angiotensin II infusion in rats. *Am J Physiol Heart Circ Physiol* 2007;292:H1685–H1689. [PubMed: 17220186]



- (15). Emmert-Buck MR, Bonner RF, Smith PD, Chuaqui RF, Zhuang Z, Goldstein SR, Weiss RA, Liotta LA. Laser capture microdissection. *Science* 1996;274:998–1001. [PubMed: 8875945]
- (16). Curran S, McKay JA, McLeod HL, Murray GI. Laser capture microscopy. *Mol Pathol* 2000;53:64–68. [PubMed: 10889904]
- (17). Fend F, Raffeld M. Laser capture microdissection in pathology. *J Clin Pathol* 2000;53:666–672. [PubMed: 11041055]
- (18). Tojo A, Gross SS, Zhang L, Tisher CC, Schmidt HHHW, Wilcox CS, Madsen KM. Immunocytochemical localization of distinct isoforms of nitric oxide synthase in the juxtaglomerular apparatus of the kidney. *J Am Soc Nephrol* 1994;4:1438–1447. [PubMed: 7512831]
- (19). Yang T, Park JM, Arend L, Huang Y, Topaloglu R, Pasumarthy A, Praetorius H, Spring K, Briggs JP, Schnermann J. Low chloride stimulation of prostaglandin E<sub>2</sub> release and cyclooxygenase-2 expression in a mouse macula densa cell line. *J Biol Chem* 2000;275:37922–37929. [PubMed: 10982805]
- (20). Paliege A, Mizel D, Medina C, Pasumarthy A, Huang YG, Bachmann S, Briggs JP, Schnermann JB, Yang T. Inhibition of nNOS expression in the macula densa by COX-2-derived prostaglandin E(2). *Am J Physiol Renal Physiol* 2004;287:F152–F159. [PubMed: 15010356]
- (21). He H, Podymow T, Zimpelmann J, Burns KD. NO inhibits Na<sup>+</sup>-K<sup>+</sup>-2Cl<sup>-</sup> cotransport via a cytochrome P-450-dependent pathway in renal epithelial cells (MMDD1). *Am J Physiol Renal Physiol* 2003;284:F1235–F1244. [PubMed: 12582005]
- (22). Cifuentes ME, Rey FE, Carretero OA, Pagano PJ. Upregulation of p67<sup>phox</sup> and gp91<sup>phox</sup> in aortas from angiotensin II-infused mice. *Am J Physiol Heart Circ Physiol* 2000;279:H2234–H2240. [PubMed: 11045958]
- (23). Lieberthal W, Triaca V, Koh JS, Pagano PJ, Levine JS. Role of superoxide in apoptosis induced by growth factor withdrawal. *Am J Physiol* 1998;275:F691–F702. [PubMed: 9815127]
- (24). Pagano PJ, Ito Y, Tornheim K, Gallop PM, Tauber AI, Cohen RA. An NADPH oxidase superoxide-generating system in the rabbit aorta. *Am J Physiol* 1995;268:H2274–H2280. [PubMed: 7611477]
- (25). Liu R, Carretero OA, Ren Y, Wang H, Garvin JL. Intracellular pH regulates superoxide production by the macula densa. *Am J Physiol Renal Physiol* 2008;295:F851–F856. [PubMed: 18667487]
- (26). Navar, LG. The regulation of glomerular filtration rate in mammalian kidneys. In: Andreoli, TE.; Hoffman, JF.; Fanestil, DD., editors. *Physiology of Membrane Disorders*. Plenum Press; New York: 1978. p. 593–627.
- (27). Schnermann J, Levine DZ. Paracrine factors in tubuloglomerular feedback: adenosine, ATP, and nitric oxide. *Annu Rev Physiol* 2003;65:501–529. [PubMed: 12208992]
- (28). Suh Y-A, Arnold RS, Lassegue B, Shi J, Xu X, Sorescu D, Chung AB, Griendling KK, Lambeth JD. Cell transformation by the superoxide-generating oxidase Mox1 [letter]. *Nature* 1999;401:79–82. [PubMed: 10485709]
- (29). Banfi B, Maturana A, Jaconi S, Arnaudeau S, Laforge T, Sinha B, Ligeti E, Demaurex N, Krause KH. A mammalian H<sup>+</sup> channel generated through alternative splicing of the NADPH oxidase homolog NOH-1. *Science* 2000;287:138–142. [PubMed: 10615049]
- (30). Touyz RM, Chen X, Tabet F, Yao G, He G, Quinn MT, Pagano PJ, Schiffrin EL. Expression of a functionally active gp91<sup>phox</sup>-containing neutrophil-type NAD(P)H oxidase in smooth muscle cells from human resistance arteries. Regulation by angiotensin II. *Circ Res* 2002;90:1205–1213. [PubMed: 12065324]
- (31). Kikuchi H, Hikage M, Miyashita H, Fukumoto M. NADPH oxidase subunit, gp91(phox) homologue, preferentially expressed in human colon epithelial cells. *Gene* 2000;254:237–243. [PubMed: 10974555]
- (32). Geiszt M, Kopp JB, Vármai P, Leto TL. Identification of Renox, an NAD(P)H oxidase in kidney. *Proc Natl Acad Sci USA* 2000;97:8010–8014. [PubMed: 10869423]
- (33). Shiose A, Kuroda J, Tsuruya K, Hirai M, Hirakata H, Naito S, Hattori M, Sakaki Y, Sumimoto H. A novel superoxide-producing NAD(P)H oxidase in kidney. *J Biol Chem* 2001;276:1417–1423. [PubMed: 11032835]

- (34). Banfi B, Molnar G, Maturana A, Steger K, Hegedus B, Demaurex N, Krause KH. A Ca(2+)-activated NADPH oxidase in testis, spleen, and lymph nodes. *J Biol Chem* 2001;276:37594–37601. [PubMed: 11483596]
- (35). De Deken X, Wang D, Many MC, Costagliola S, Libert F, Vassart G, Dumont JE, Miot F. Cloning of two human thyroid cDNAs encoding new members of the NADPH oxidase family. *J Biol Chem* 2000;275:23227–23233. [PubMed: 10806195]
- (36). Dupuy C, Ohayon R, Valent A, Noel-Hudson MS, Deme D, Virion A. Purification of a novel flavoprotein involved in the thyroid NADPH oxidase. Cloning of the porcine and human cDNAs. *J Biol Chem* 1999;274:37265–37269. [PubMed: 10601291]
- (37). Edens WA, Sharling L, Cheng G, Shapira R, Kinkade JM, Lee T, Edens HA, Tang X, Sullards C, Flaherty DB, Benian GM, Lambeth JD. Tyrosine cross-linking of extracellular matrix is catalyzed by Duox, a multidomain oxidase/peroxidase with homology to the phagocyte oxidase subunit gp91phox. *J Cell Biol* 2001;154:879–891. [PubMed: 11514595]
- (38). Hilenski LL, Clempus RE, Quinn MT, Lambeth JD, Griendling KK. Distinct subcellular localizations of Nox1 and Nox4 in vascular smooth muscle cells. *Arterioscler Thromb Vasc Biol* 2004;24:677–683. [PubMed: 14670934]
- (39). van Buul JD, Fernandez-Borja M, Anthony EC, Hordijk PL. Expression and localization of NOX2 and NOX4 in primary human endothelial cells. *Antioxid Redox Signal* 2005;7:308–317. [PubMed: 15706079]
- (40). Terada LS. Specificity in reactive oxidant signaling: think globally, act locally. *J Cell Biol* 2006;174:615–623. [PubMed: 16923830]
- (41). Martyn KD, Frederick LM, von LK, Dinauer MC, Knaus UG. Functional analysis of Nox4 reveals unique characteristics compared to other NADPH oxidases. *CELL SIGNAL* 2006;18:69–82. [PubMed: 15927447]
- (42). Cardounel AJ, Xia Y, Zweier JL. Endogenous methylarginines modulate superoxide as well as nitric oxide generation from neuronal nitric-oxide synthase: differences in the effects of monomethyl- and dimethylarginines in the presence and absence of tetrahydrobiopterin. *J Biol Chem* 2005;280:7540–7549. [PubMed: 15574418]

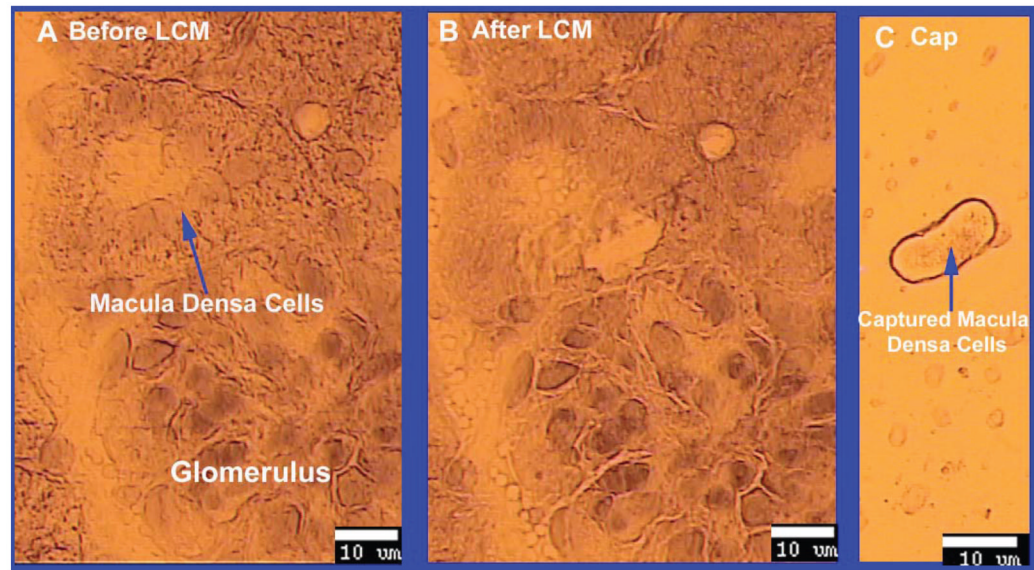


**Fig 1. Isolating macula densa cells with laser capture microdissection (LCM)**

A. Macula densa cells were identified by their anatomical location and morphology with the LCM microscope in a frozen slide of kidney cortex from SD rat. B. Macula densa were captured with LCM, using a beam width of 7.5 μm and a beam intensity of 50 mW. C. Captured macula densa cells on the cap.

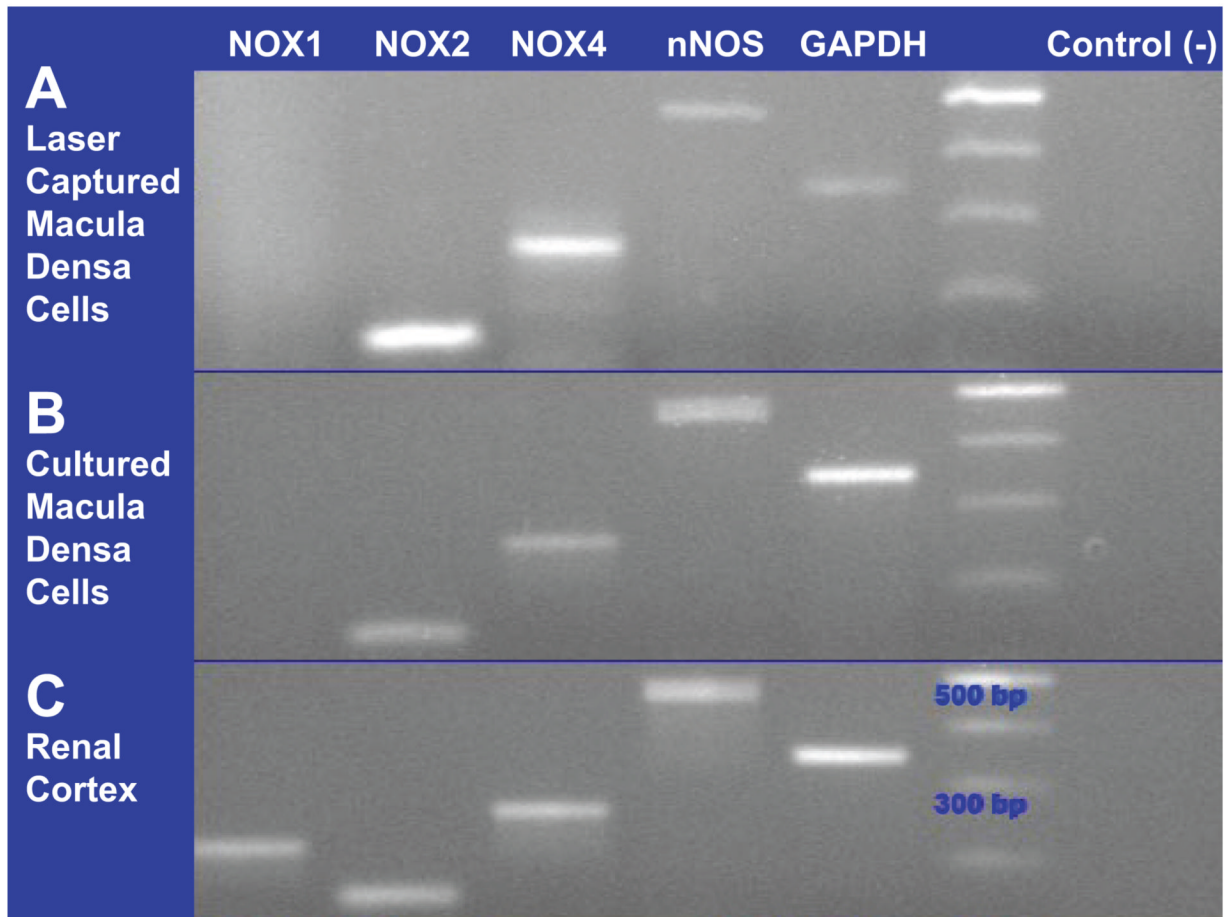


**Fig 2. Isoforms of NADP(H) oxidase expressed by the macula densa identified by RT-PCR**

A. NOX2 and NOX4 are detected in laser captured macula densa cells. nNOS as a positive marker of the macula densa cells. B. In cultured macula densa cells (MMDD1), NOX2, NOX4 and nNOS are detected. C. All primers were tested in renal cortex.

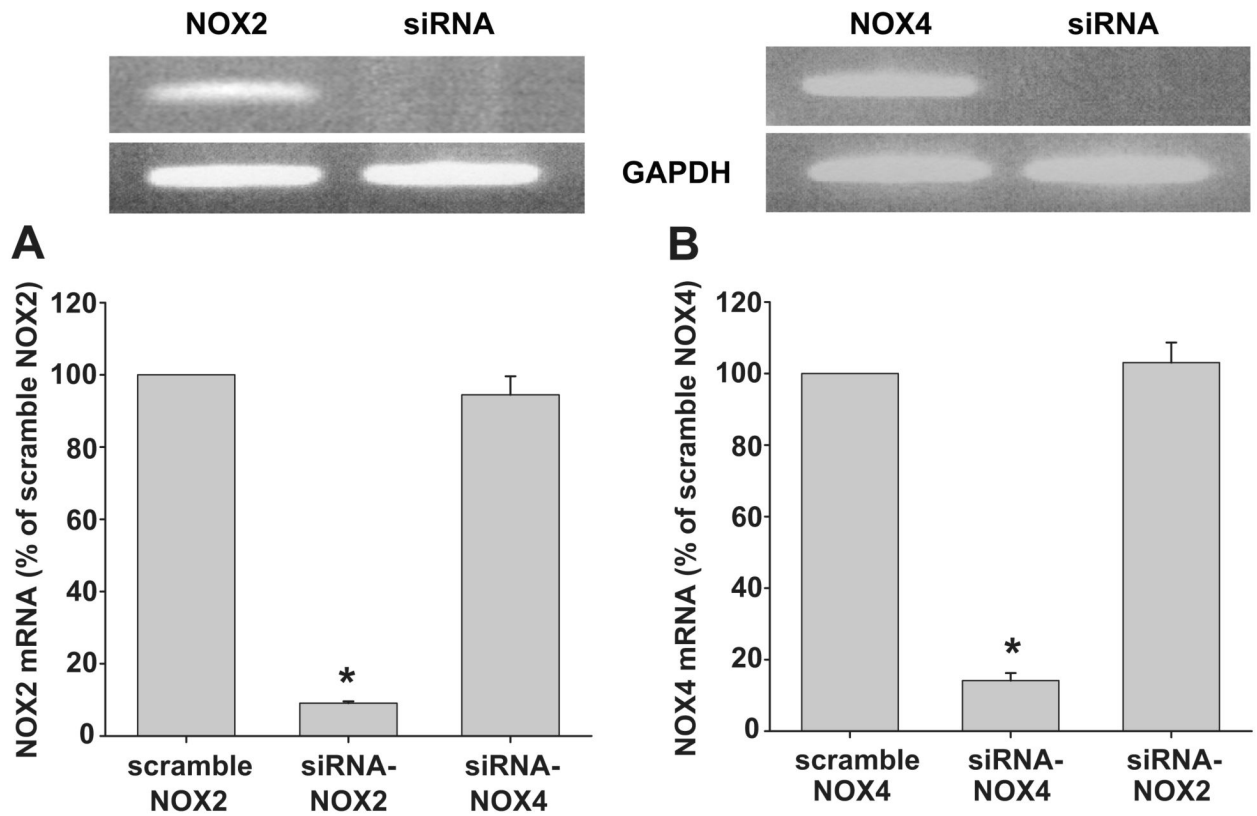


**Fig 3. siRNA knocking down NOX2 and NOX4 mRNA**

Top: representative RT-PCR of scrambled and siRNA NOX2 and NOX4. Bottom: quantitative densitometry of the bands (n = 5; \* p < 0.01).

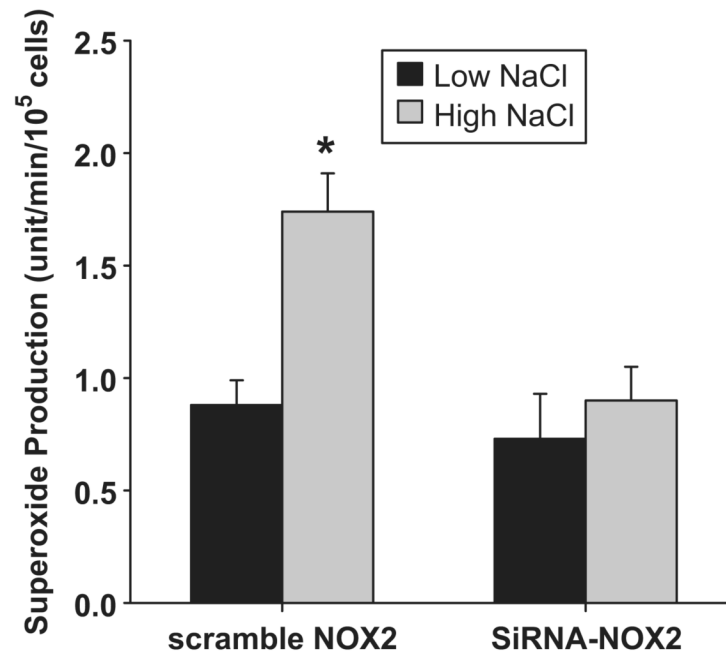


**Fig 4. Effect of silencing NOX2 on superoxide concentration induced by NaCl**  
High NaCl induced significant superoxide production in cells treated with scrambled siRNA. This superoxide production was blocked in cells treated with NOX2 siRNA.

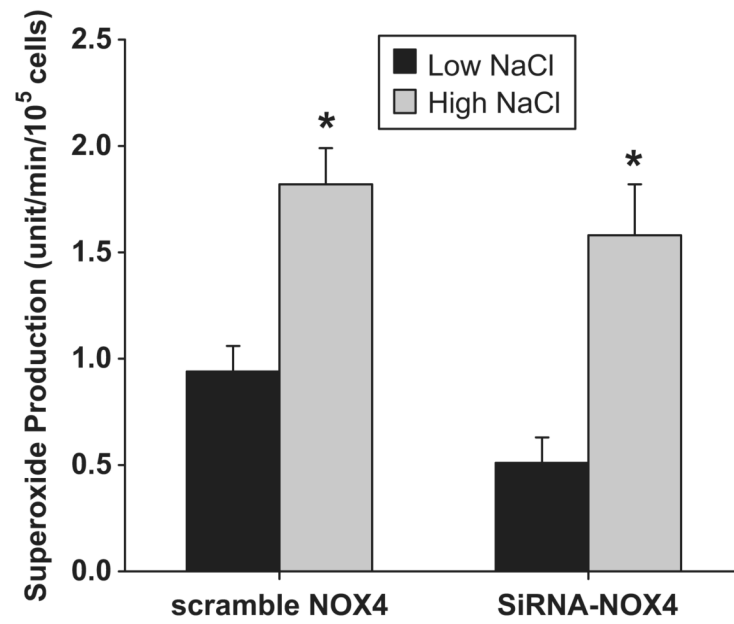


**Fig 5. Effect of knocking down NOX4 on superoxide concentration induced by NaCl**  
High NaCl induced significant superoxide production in cells treated with either scrambled siRNA or NOX4 siRNA. Basal superoxide production was blunted in cells treated with NOX4 siRNA compared with control.

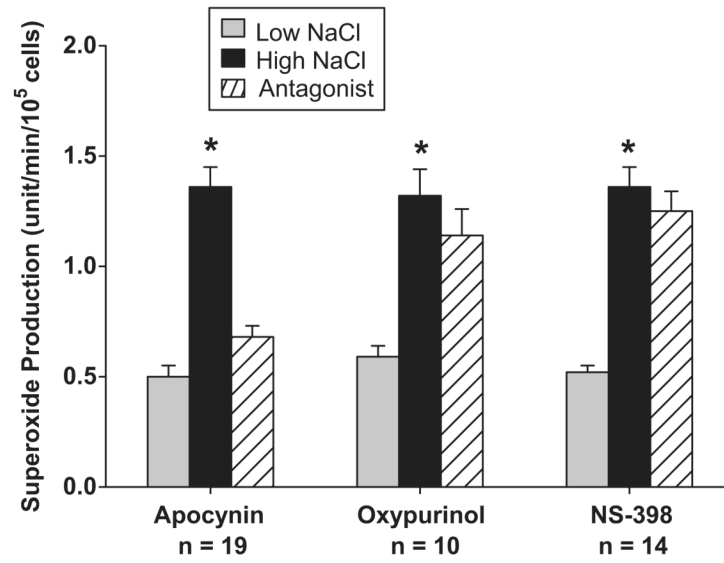


**Fig 6.** Contributions of NAD(P)H oxidase, xanthine oxidase and COX-2 to  $O_2^-$  production induced by NaCl.



**Table 1**  
Primer sequences, expected band and GenBank numbers

Gene	Primer sequence	GenBank #	PCR length (bp)
NOX1	F: 5'-tgaacaacagcactcaccaatgcc -3' R: 5'-agttgtgaaccaggcaaaggcac -3'	NM_053683	245
NOX2	F: 5'-ccagtgaagatgtgttcagct-3' R: 5'-gcacagccagtagaagtagat-3'	AF298656	155
NOX4	F: 5'-accagatgttggcctaggattgt -3' R: 5'-agttcactgagaagttcagggcgt -3'	NM_053524	261
nNOS	F: 5'-cttccgaagcttctggcaacagcgacaatt-3' R: 5'-ggactcagatctaaggcgttggtcacttc-3'	NM_052799.1	472
GAPDH	F: 5'-catcctgcaccaccaactgcttag -3' R: 5'-gcctgcttaccaccttctgatg-3'	NM_017008	346